

## Unified Mechanistic Concept of Electrophilic Aromatic Nitration: Convergence of Computational Results and Experimental Data

Pierre M. Esteves,<sup>\*,†,‡,⊥</sup> José Walkimar de M. Carneiro,<sup>§</sup> Sheila P. Cardoso,<sup>§</sup> André G. H. Barbosa,<sup>‡</sup> Kenneth K. Laali,<sup>||</sup> Golam Rasul,<sup>†</sup> G. K. Surya Prakash,<sup>†</sup> and George A. Olah<sup>\*,†</sup>

*Contribution from the Loker Hydrocarbon Research Institute and Department of Chemistry, University of Southern California, Los Angeles, California 90089-1661, Instituto de Química, Universidade Federal do Rio de Janeiro, Cidade Universitária CT Bloco A, 21949-900, Rio de Janeiro, Brazil, Instituto de Química, Universidade Federal Fluminense, Outeiro de São João Batista, s/n, 24020-150 Niterói, Rio de Janeiro, Brazil, and Department of Chemistry, Kent State University, Kent, Ohio 44242*

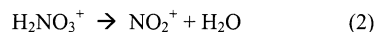
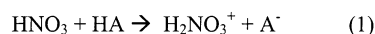
Received October 29, 2002; Revised Manuscript Received December 23, 2002; E-mail: pesteves@iq.ufrrj.br or olah@usc.edu

**Abstract:** The mechanism of electrophilic aromatic nitration was revisited. Based on the available experimental data and new high-level quantum chemical calculations, a modification of the previous reaction mechanism is proposed involving three separate intermediates on the potential energy diagram of the reaction. The first, originally considered an unoriented  $\pi$ -complex or electron donor acceptor complex (EDA), involves high electrostatic and charge-transfer interactions between the nitronium ion and the  $\pi$ -aromatics. It explains the observed low substrate selectivity in nitration with nitronium salts while maintaining high positional selectivity, as well as observed oxygen transfer reactions in the gas phase. The subsequent second intermediate originally considered an oriented " $\pi$ -complex" is now best represented by an intimate radical cation–molecule pair,  $C_6H_6^+ \cdot / NO_2$ , that is, a SET complex, indicative of single-electron transfer from the aromatic  $\pi$ -system to  $NO_2^+$ . Subsequently, it collapses to afford the final  $\sigma$ -complex intermediate, that is, an arenium ion. The proposed three discrete intermediates in electrophilic aromatic nitration unify previous mechanistic proposals and also contribute to a better understanding of this fundamentally important reaction. The previously obtained ICR data of oxygen transfer from  $NO_2^+$  to the aromatic ring are also accommodated by the proposed mechanism. The most stable intermediate of this reaction on its potential energy surface is a complex between phenol and  $NO^+$ . The phenol· $NO^+$  complex decomposes affording  $C_6H_6O^+ \cdot / PhOH^+$  and  $NO$ , in agreement with the ICR results.

### Introduction

Electrophilic aromatic substitution<sup>1</sup> and nitration in particular<sup>2</sup> have been among the most intensively studied organic reactions. They have played a key role in the study of aromatic reactivity and selectivity.<sup>3</sup> Although aromatic nitration is commonly referred to as a "typical" example of a mechanistically well-defined reaction,<sup>4</sup> important mechanistic aspects are still evolving.<sup>5–7</sup> The fundamental mechanism of electrophilic nitra-

### Scheme 1. Ingold–Hughes Mechanism for Electrophilic Aromatic Nitration



tion was elucidated by Ingold and Hughes<sup>3,8</sup> (Scheme 1). Accordingly, the nitration reaction involves the  $NO_2^+$  cation as the reactive electrophile, which is responsible for attack on the aromatic compound. It forms  $ArHNO_2^+$ , the Wheland intermediate, which was subsequently identified as a  $\sigma$ -complex or an arenium ion. The focal point of still ongoing studies and

<sup>†</sup> University of Southern California.

<sup>‡</sup> Universidade Federal do Rio de Janeiro.

<sup>§</sup> Universidade Federal Fluminense.

<sup>||</sup> Kent State University.

<sup>⊥</sup> Permanent address: Instituto de Química, Universidade Federal do Rio de Janeiro, Cidade Universitária CT Bloco A, 21949-900, Rio de Janeiro, Brazil.

- (1) (a) Considered as Electrophilic Aromatic Substitution, Part 67. For part 66, see: Salzbrunn, D.; Simon, J.; Prakash, G. K. S.; Petasis, N. A.; Olah, G. A. *Synlett* **2000**, 10, 1485. (b) Taylor, R. *Electrophilic Aromatic Substitution*; John Wiley & Sons: Chichester, U.K., 1990.
- (2) (a) Olah, G. A.; Malhotra, R.; Narang, S. C. *Nitration Methods and Mechanisms*; VCH: New York, 1989. (b) Cardoso, S. P.; Carneiro, J. W. M. *Quím. Nova* **2001**, 24, 381–389.
- (3) Ingold, C. K. *Structure and Mechanism in Organic Chemistry*; Cornell University Press: New York, 1969.

(4) (a) March, J. *Advanced Organic Chemistry*; John Wiley & Sons: New York, 1985. (b) Lowry, T. H.; Richardson, K. S. *Mechanism and Theory in Organic Chemistry*; Harper and Row: New York, 1987.

(5) Aschi, M.; Attinà, M.; Cacace, F.; Ricci, A. *J. Am. Chem. Soc.* **1994**, 116, 9535.

(6) Peluso, A.; Del Re, G. *J. Phys. Chem.* **1996**, 100, 5303.

(7) Lund, T.; Ebersson, L. *J. Chem. Soc., Perkin Trans. 2* **1997**, 1435.

(8) Ingold, C. K.; Hughes, E. D. *J. Chem. Soc.* **1950**, 2400.

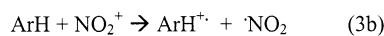
**Scheme 2**. Olah's Modified Mechanism for Electrophilic Aromatic Nitration

discussions is the possible role of a discrete additional earlier intermediate,  $\pi$ -complex formation or single-electron transfer (SET) step on the reaction coordinate, as contrasted with direct two-electron-transfer electrophilic addition (polar addition), leading to a  $\sigma$ -complex intermediate.<sup>9</sup>

Aromatic nitration is most commonly carried out as an acid-catalyzed reaction between the aromatic substrate and nitric acid (or its derivatives). According to the Ingold–Hughes mechanism,  $\text{HNO}_3$  forms the nitronium ion ( $\text{NO}_2^+$ ) in the presence of a strong acid. This ion then reacts further with the aromatic substrate to form an arenium ion in a rate-determining step, which in a subsequent step undergoes proton elimination leading to the nitrated product (Scheme 1). Early experiments firmly established  $\text{NO}_2^+$  as the key electrophile.<sup>3</sup> It was also agreed that the stability of the arenium ion intermediate determines the positional selectivity (regioselectivity) of the nitrated products.

A modification of the original Ingold–Hughes mechanism was proposed by Olah and co-workers, who suggested the existence of a separate intermediate prior to the subsequent formation of the arenium ion (Scheme 2).<sup>10–13</sup> This first intermediate was necessary in order to explain the low substrate selectivity observed in nitration of aromatics with the nitronium salts,<sup>2,10,11</sup> such as  $\text{NO}_2^+\text{BF}_4^-$  and  $\text{NO}_2^+\text{PF}_6^-$ , despite that the positional selectivity (regioselectivity) remained high and was unaffected. This first intermediate was considered as a  $\pi$ -complex,<sup>2,10,11</sup> that is, a weakly bound state involving low, non-specific, attractive interaction between the  $\text{NO}_2^+$  ion and the aromatic  $\pi$  system as an entity. Formation of the  $\pi$ -complex in a rate-determining step,<sup>2</sup> was proposed to be responsible for the low substrate selectivity observed upon nitration of activated aromatics while retaining positional selectivity. This proposal stood in contrast with Brown's empirical selectivity rule,<sup>14,15</sup> which, however, considered a single intermediate and consequently substrate and positional selectivities are connected.

Schofield and collaborators studied the nitration of alkylbenzenes using nitric acid in 68% sulfuric acid as nitration media.<sup>12,13,16</sup> Under these reaction conditions, they observed that there is a limit to the maximum rate observed for the reaction. They concluded that the reaction rate is close to the limiting rate for diffusion of the reactive species into the reaction medium. This led them to propose that the initial complex is an encounter pair, whose rate of formation would be determined by the diffusion rate of  $\text{NO}_2^+$  in the aromatic solvent, with no bonding interaction between them. The reactants are encapsulated in the solvent cage, and random collisions lead to the

**Scheme 3**. Single-Electron-Transfer Mechanism for Electrophilic Aromatic

$\sigma$ -complex intermediate. The difference between Schofield's and Olah's mechanism is in the nature of the first intermediate. In Olah's mechanism, this intermediate was suggested to be a  $\pi$ -complex with a weak but well-defined interaction between the aromatic substrate and the nitronium ion. In Schofield's mechanism, the intermediate is an encounter pair, which does not involve any bonding interaction between the reacting species and is held together only by the solvent cage.<sup>12,16</sup> There is, however, no indication of significant solvent effects in nitration with nitronium salts. Gas-phase electrophilic nitration studied by Cacace et al.<sup>23</sup> also gave results showing low substrate but high positional selectivity under conditions where solvent cage formation cannot be involved.

In contrast with the two-electron transfer, that is, the polar electrophilic reaction mechanism, the possibility of an alternative pathway involving a one-electron-transfer pathway was invoked in subsequent years.<sup>17–20</sup> First proposed by Kenner<sup>17</sup> and Weiss,<sup>18</sup> the one-electron pathway in aromatic nitration acquired renewed interest based on the works of Perrin<sup>19</sup> on the electrochemical nitration of naphthalene. Although the general validity of the concept particularly with less nucleophilic aromatics was questioned,<sup>21</sup> it nevertheless attracted renewed attention to the single-electron-transfer (SET) pathway of aromatic nitration. This mechanism involves, after the approach of the two reactants, a single-electron-transfer step from the aromatic substrate to the nitronium ion as the initial step. It is followed by radical pair recombination between the aromatic radical cation and the  $\text{NO}_2$  radical formed,<sup>20</sup> leading to the identical arenium ion intermediate as proposed in the Ingold–Hughes mechanism (Scheme 3).

Extensive more recent work by Kochi and co-workers has further substantiated the single-electron-transfer mechanism for activated aromatics, especially through the study of electron donor–acceptor complexes, formed between aromatic substrates and nitronium ion carriers ( $\text{NO}_2\text{Y}$ ), involved in the photochemical as well as in thermal activation of aromatic nitration.<sup>20</sup> Specific absorption bands observed upon mixing the aromatic substrate with the nitronium ion carrying species ( $\text{NO}_2\text{Y}$ ) were considered to stem from a donor–acceptor complex (also called charge-transfer complex). This intermediate would involve the nitrating agent (acceptor) and the aromatic (donor). Accordingly, Kochi proposed a mechanism based on single-electron transfer (Scheme 4).

(9) Reference 2a, Chapter 3.

(10) Olah, G. A.; Kuhn, S.; Flood, S. H. *J. Am. Chem. Soc.* **1961**, *83*, 4571.

(11) Olah, G. A. *Acc. Chem. Res.* **1971**, *4*, 240.

(12) Coombes, R. D.; Moodie, R. B.; Schofield, K. *J. Chem. Soc. B* **1968**, 800.

(13) Schofield, K. *Aromatic Nitration*; Cambridge University Press: Cambridge, 1980.

(14) Johnson, C. D. *Chem. Rev.* **1975**, *75*, 755.

(15) Pross, A. *Adv. Phys. Org. Chem.* **1977**, *14*, 1977.

(16) Hoggett, J. G.; Moodie, R. B.; Schofield, K. *J. Chem. Soc. B* **1969**, 1.

(17) Kenner, J. *Nature* **1945**, *156*, 369.

(18) Weiss, J. *Trans. Faraday Soc.* **1946**, *42*, 116.

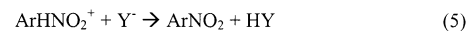
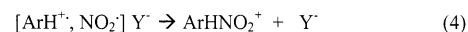
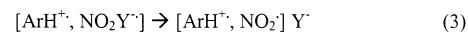
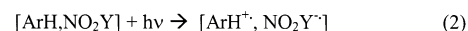
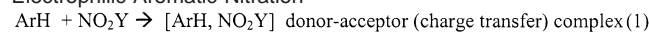
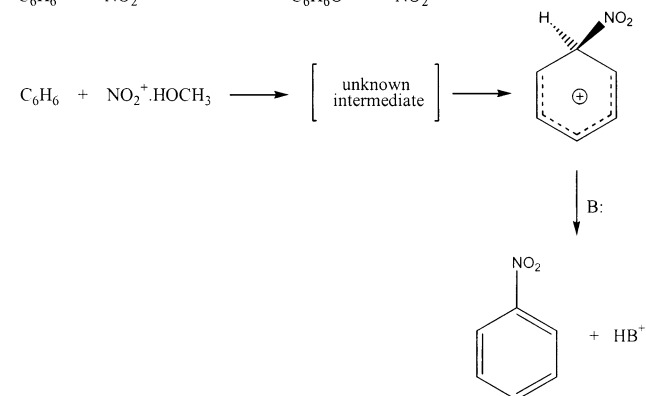
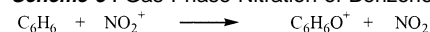
(19) Perrin, C. L. *J. Am. Chem. Soc.* **1977**, *99*, 5516.

(20) (a) Kochi, J. K. *Acc. Chem. Res.* **1992**, *25*, 39. (b) Kim, E. K.; Bockman, T. M.; Kochi, J. K. *J. Am. Chem. Soc.* **1993**, *115*, 3091 and references therein.

(21) (a) Ebersson, L.; Jönsson, L.; Radner, F. *Acta Chem. Scand. B* **1978**, *32*, 749. (b) Ebersson, L.; Radner, F. *Acta Chem. Scand. B* **1980**, *34*, 739. (c) Ebersson, L.; Radner, F. *Acc. Chem. Res.* **1987**, *20*, 53.

(22) (a) Fukuzumi, S.; Kochi, J. K. *J. Am. Chem. Soc.* **1981**, *103*, 7240. (b) Takeshita, K. *J. Chem. Phys.* **1994**, *101*, 2192. (c) Raghavachari, K.; Haddon, R. C.; Miller, T. A.; Bondbey, V. E. *J. Chem. Phys.* **1983**, *79*, 1387. (d) Attinà, M.; Cacace, F.; Ricci, A. *J. Phys. Chem.* **1996**, *100*, 4424–4429.

(23) (a) Attinà, M.; Cacace, F.; Yanez, M. *J. Am. Chem. Soc.* **1987**, *109*, 5092. (b) Aschi, M.; Attinà, M.; Cacace, F.; Ricci, A. *J. Am. Chem. Soc.* **1994**, *116*, 9535. (c) Attinà, M.; Cacace, F.; de Petris, G. *Angew. Chem., Int. Ed. Engl.* **1987**, *26*, 1177. (d) Cacace, F. *Acc. Chem. Res.* **1988**, *21*, 215.

**Scheme 4.** Kochi's Single-Electron-Transfer Mechanism for Electrophilic Aromatic Nitration**Scheme 5.** Gas-Phase Nitration of Benzene

The rate-determining step in this mechanism is the formation of the ion pair  $[\text{ArH}^+, \text{NO}_2\text{Y}^-]$ , that is, step 2, which defines the substrate selectivity. The positional selectivity (regioselectivity) is determined by the spin density in the aromatic cation radical ( $\text{ArH}^+$ ), this being the driving force for the collapse of the  $[\text{ArH}^+, \text{NO}_2]$  complex into the  $\sigma$ - (Wheland) intermediate. Concerns about this mechanism are that the rates of reaction estimated by Marcus theory are much lower than the rates observed in solution and the high energy needed for abstracting an electron from the  $6\pi$ -aromatic benzene (or the more deactivated aromatics). With highly reactive electron-rich aromatic substrates, however, the energetics can become favorable. Another question to be raised relates to the low observed *ipso*-substitution, which contrasts with the high spin density on that position.<sup>22</sup>

Ion–molecule reactions in the gas phase using ion cyclotron resonance spectroscopy (ICR) demonstrated that the reaction of  $\text{NO}_2^+$  with benzene does not lead to a nitrated product but to  $\text{C}_6\text{H}_6\text{O}^+$  (Scheme 5). This points to the ambident electrophilic character of the nitronium ion, since it could react via either the oxygen or the nitrogen atoms. On the other hand, if an  $\text{NO}_2^+$  carrier (“complexed”  $\text{NO}_2^+$ ) such as  $\text{CH}_3\text{OH}-\text{NO}_2^+$  and  $\text{CH}_2\text{O}-\text{NO}_2^+$  is used as the nitrating agent under similar gas-phase conditions, nitration occurs affording products with a similar positional selectivity observed for the reaction in the condensed phase.<sup>23</sup> In these reactions, two intermediates are indicated. The first is of a yet unknown structure which is then converted into the second intermediate of arenium ion ( $\sigma$ -complex) nature. This contrasts with the solvent cage mechanism of Schofield, since there is no solvent involved in these gas-phase reactions.

Varied quantum mechanical and ab initio studies were also applied to study the mechanism of the aromatic nitration.<sup>6,24–27</sup>

(24) Szabó, K. J.; Hornfeldt, A.-B.; Gronowitz, S. *J. Am. Chem. Soc.* **1992**, *114*, 6827.

Early theoretical studies aimed at clarifying the nature of the initial complex gave no clear indications. Hartree–Fock calculations on the potential energy surface of the approach of the  $\text{NO}_2^+$  ion to benzene led directly to the arenium ion, without an activation barrier.<sup>20,24</sup> An initial  $\pi$ -complex form was found only upon restricted optimization<sup>25</sup> or by calculating a solvated nitronium ion (protonated methyl nitrate).<sup>24</sup> Subsequent work was stimulated by the gas-phase studies.<sup>23a,28–30</sup> Most recent and more accurate calculations showed that there is a crossing of electronic potential energy surfaces in the approach of the  $\text{NO}_2^+$  to the aromatic cation.<sup>6,26,27</sup> This crossing of electronic states (also known as conical intersection<sup>31</sup>) can be interpreted as the transition of the ground state of the aromatic–nitronium ion complex ( $|\text{ArH}, \text{NO}_2^+\rangle$ ) to the aromatic cation–neutral  $\text{NO}_2$  ( $|\text{ArH}^+, \text{NO}_2^*\rangle$ ) complex, which is in accord with the single-electron-transfer mechanism. Recent ab initio molecular dynamics calculations at the MRCI level indicated that the activation barrier for the electron transfer may be as small as 3.3 kcal/mol.<sup>26</sup> This is significant considering the rather high first ionization potential of benzene and substituted benzenes (vide supra).

Previous mechanistic proposals agree that in principle two intermediates are involved in electrophilic aromatic nitration, the latter being unquestionably an arenium ion (the  $\sigma$ -complex). Differing pathways lead subsequently to the same arenium intermediate. Deprotonation of the arenium ion has always been considered to be a fast process, since no primary hydrogen isotopic effect was observed.<sup>32</sup> The still unanswered question is the nature of the first intermediate, especially in the case of reactions involving less active or deactivated aromatics. The linear nitronium ion has no empty atomic orbital on nitrogen but is polarizable as the approaching aromatic displaces an electron pair from an  $\text{N}=\text{O}$  bond onto the oxygen, developing an empty orbital on nitrogen. Is the reaction driven by direct (polar) addition of the  $\text{NO}_2^+$  ion to the aromatic nucleophile involving a two-electron process or is it a single-electron-transfer process from the aromatic substrate to  $\text{NO}_2^+$ ? While experimental data do not converge clearly to any one proposal,<sup>6,7,20,33,34</sup> theoretical studies which mainly considered possible single-electron transfer concluded that this is the preferable mechanism, at least for substrates more activated (electron rich) than benzene.<sup>6,26</sup>

A useful distinction between single- and two-electron (polar) transfer is that, in the first case, according to the Franck–Condon principle, the overlap between the vibrational wave functions associated to donor and acceptor moieties does not change much in the process of electron transfer. In other words, there is no significant bond distance and/or angle accommoda-

(25) Politzer, P.; Jayasuriya, K.; Sjöberg, P.; Laurence, P. R. *J. Am. Chem. Soc.* **1985**, *107*, 1174.

(26) Alburnia, A. R.; Borrelli, R.; Peluso, A. *Theor. Chem. Acc.* **2000**, *104*, 218–222.

(27) Feng, J.; Zheng, X.; Zemer, M. C. *J. Org. Chem.* **1986**, *51*, 4531.

(28) Benezra, S. A.; Hoffman, M. K.; Bursley, M. M. *J. Am. Chem. Soc.* **1970**, *92*, 7501.

(29) Morrison, J. D.; Stanney, K.; Tedder, J. M. *J. Chem. Soc., Perkin Trans. 2* **1981**, 967.

(30) Dunbar, R. C.; Shen, J.; Olah, G. A. *J. Am. Chem. Soc.* **1972**, *94*, 6862–6864.

(31) Yarkony, D. R. *J. Phys. Chem.* **1996**, *100*, 18612–18628.

(32) Melander, L. *Isotope Effects on Reaction Rates*; Ronald Press: New York, 1960.

(33) Kim, E. K.; Lee, K. Y.; Kochi, J. K. *J. Am. Chem. Soc.* **1992**, *114*, 1576.

(34) Ebersson, L.; Hartshorn, M. P.; Radner, F. *Acta Chem. Scand.* **1994**, *48*, 937.

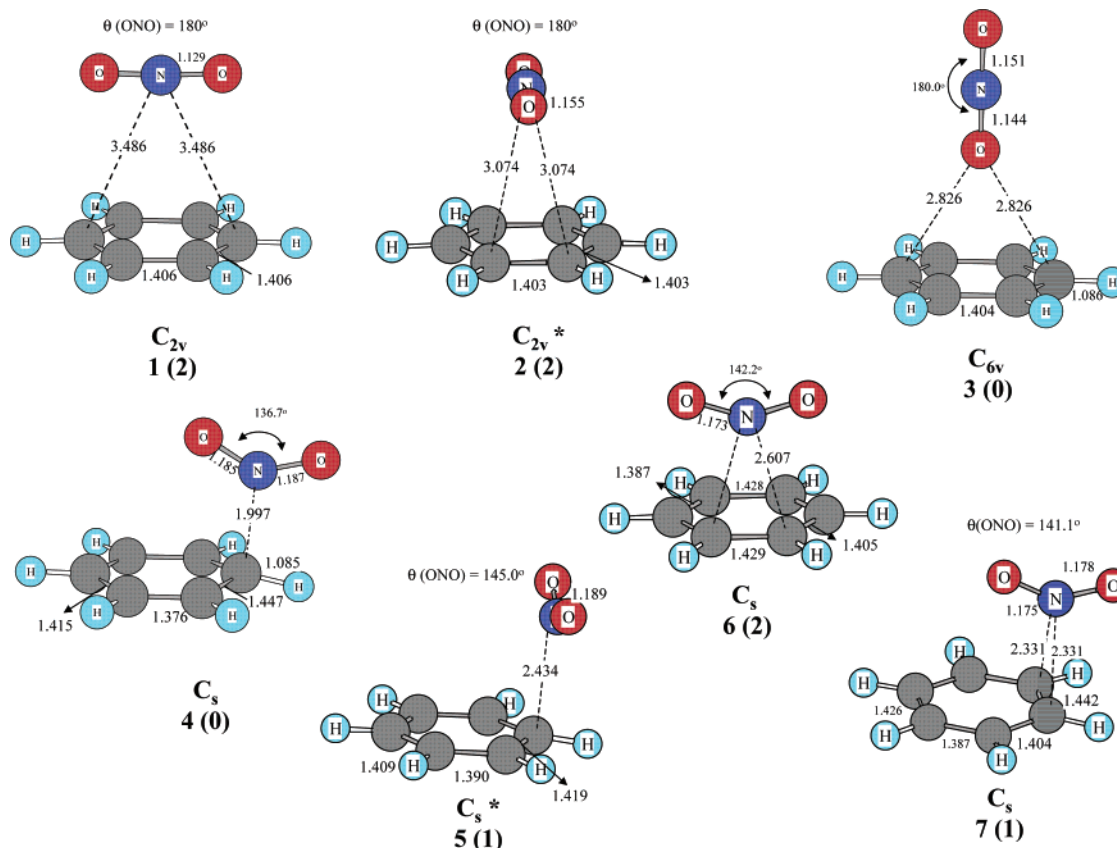


**Figure 1.** Geometries for  $\text{NO}_2^+$ /benzene complexes **1–7** obtained with energy minimization procedures at the B3LYP/6-31++G\*\* level.

tion for the new species. In the second case, the bonds involved in the reaction change concomitantly with the electron transferred from one reactant to the other. At some point, the single-electron transfer and the two-electron (polar) mechanism merge, since they represent the two extremes of a possible continuum.

To investigate in more detail the still challenging problem of the mechanism of electrophilic nitration of aromatics, we carried out detailed quantum chemical calculations of the reaction of  $\text{NO}_2^+$  with selected aromatics. For comparison, similar calculations were also performed with representative olefins.

## Results and Discussion

To study the electrophilic nitration of aromatics, we directed our investigations primarily to the study of the interaction of  $\text{NO}_2^+$  with benzene. Several isomeric structures were found to be minima on the potential energy surface of the reaction. A number of additional structures were also found and characterized as transition states for the interconversion among the located minima. Geometries for these, obtained after energy minimization procedures, are shown in Figures 1–6.

Structures **1–7** correspond to various ways by which  $\text{NO}_2^+$  can approach the  $\pi$ -system of benzene. Structures **8–27** correspond to possible products formed via the reaction of  $\text{NO}_2^+$  with benzene. The structures **5, 7, 9–11, 15, 19, 22**, and **28–37** correspond to transition states connecting the formed intermediates.

A total of 16 structures were found to be minima on the potential energy surface. Table 1 summarizes the relative energies for the species investigated, as well as related species of interest. Figure 7 is a representation of the potential energy

**Table 1.** B3LYP/6-311++G\*\*/B3LYP/6-31++G\*\* Relative Energies (298.15 K and 1 atm) for the Interaction of Benzene with  $\text{NO}_2^+$

species	$\Delta H$ (298 K) (kcal/mol)	species	$\Delta H$ (298 K) (kcal/mol)
<b>1</b>	17.71	<b>23</b>	−4.38
<b>2</b>	22.71 <sup>a</sup>	<b>24</b>	−5.72
<b>3</b>	14.30	<b>25</b>	−3.93
<b>4</b>	0.73	<b>26</b>	−24.71
<b>5</b>	9.68 <sup>a</sup>	<b>27</b>	−32.81
<b>6</b>	7.50	<b>28</b>	10.82
<b>7</b>	1.12	<b>29</b>	5.84
<b>8</b>	0.00	<b>30</b>	5.94
<b>9</b>	5.77 <sup>a</sup>	<b>31</b>	17.22
<b>10</b>	1.56	<b>32</b>	22.81
<b>11</b>	8.63	<b>33</b>	12.49
<b>12</b>	6.55	<b>34</b>	14.20
<b>13</b>	5.51	<b>35</b>	20.15
<b>14</b>	−5.96	<b>36</b>	7.74
<b>15</b>	−7.67	<b>34</b>	8.26
<b>16</b>	11.97	$\text{NO}_2^+ + \text{C}_6\text{H}_6$	33.54
<b>17</b>	16.45	$\text{NO}_2^+ + \text{C}_6\text{H}_6^+$	11.70
<b>18</b>	14.58	$\text{NO}^+ + \text{C}_6\text{H}_6\text{O}^+$	35.76
<b>19</b>	5.22	$\text{C}_6\text{H}_6\text{NO}_2 + \text{H}^+$	159.41
<b>20</b>	30.36	$\text{PhOH} + \text{NO}^+$	4.27
<b>21</b>	−47.02	$\text{PhOH}^+ + \text{NO}$	−29.74
<b>22</b>	11.18		

<sup>a</sup> B3LYP/6-311++G\*\*//MP2(full)/6-31++G\*\*.

surface of the reaction of  $\text{NO}_2^+$  with benzene in the gas phase, where the main reaction intermediates and possible pathways interconnecting them are shown. It can be seen that the most stable species on this potential energy surface is the complex  $[\text{PhOH}\cdot\text{NO}]^+$  (**21**), followed, in order of stability, by O-protonated nitrobenzene and the  $\sigma$ -complex in which an oxygen atom is transferred to the aromatic ring (structure **15**), as well

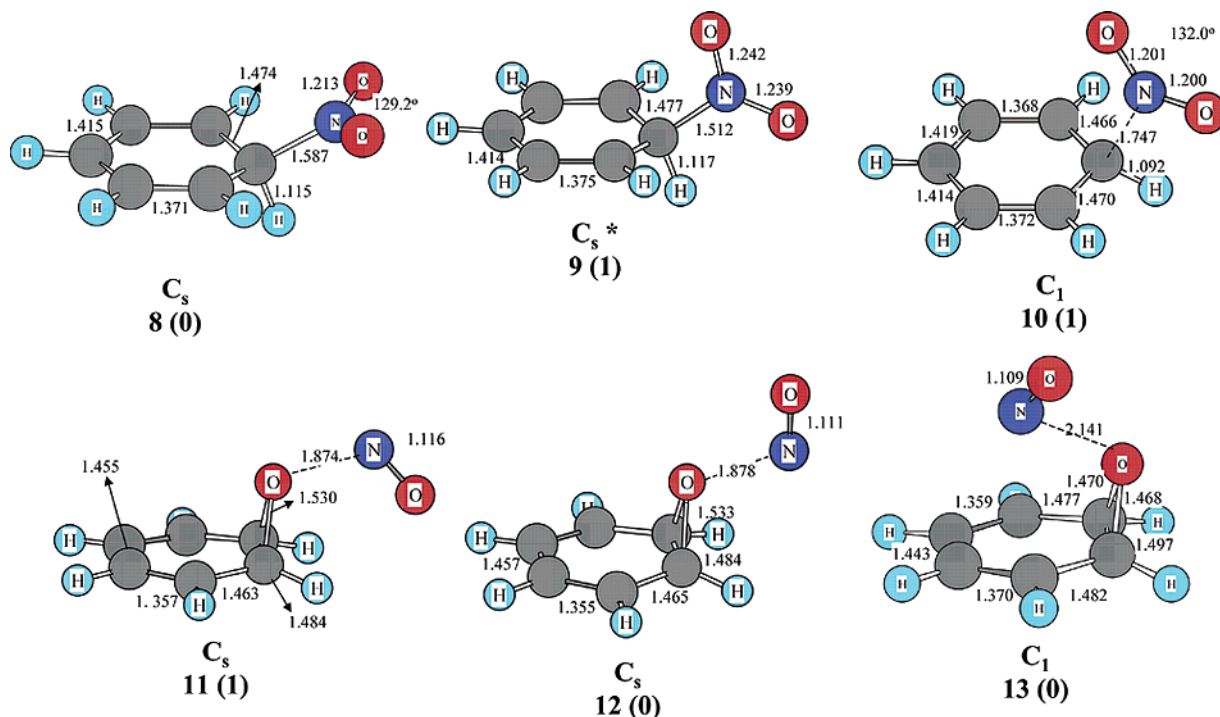


**Figure 2.** Geometries for products 8–13 of  $\text{NO}_2^+$ /benzene obtained with energy minimization procedures at the B3LYP/6-31++G\*\* level.

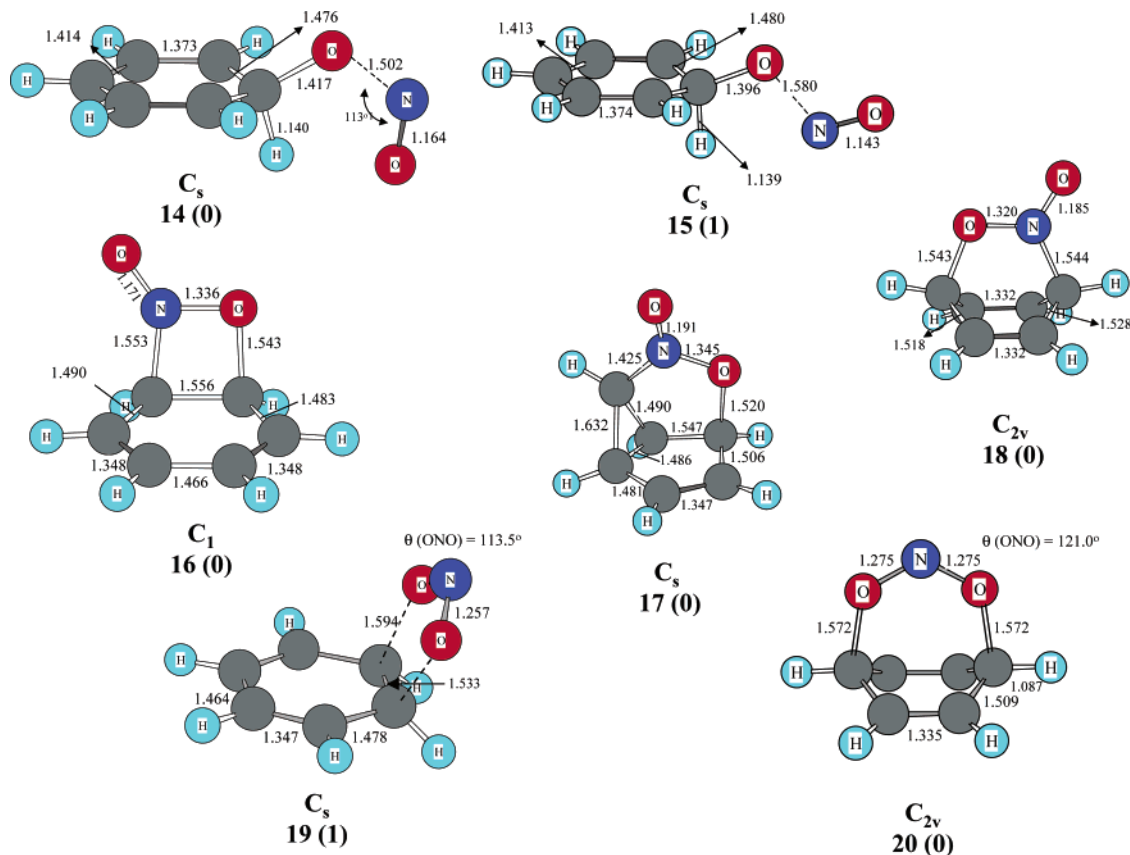


**Figure 3.** Geometries for products 14–20 of  $\text{NO}_2^+$ /benzene obtained with energy minimization procedures at the B3LYP/6-31++G\*\* level.

as other  $\sigma$ -complexes of C-protonation of nitrobenzene (**21**, **22**, **23**) and the nitrobenzenium ion  $\sigma$ -complex **8**, respectively.

The calculational data obtained allow a better rationalization of the mechanistic aspects of the electrophilic nitration of benzene with the nitronium ion. Nitrobenzene is the main reaction product when the reaction involves solvated nitronium

ion species,<sup>23</sup> while oxygen ( $\text{O}^+$ ) transfer to benzene is observed under gas-phase ion–molecule reaction conditions, wherein no solvent effects are involved.

Among the possible reaction intermediates (minima on the potential energy surface), the structures **3**, **4**, **8**, **26**, and **27** are of primary interest for the understanding of the mechanism of

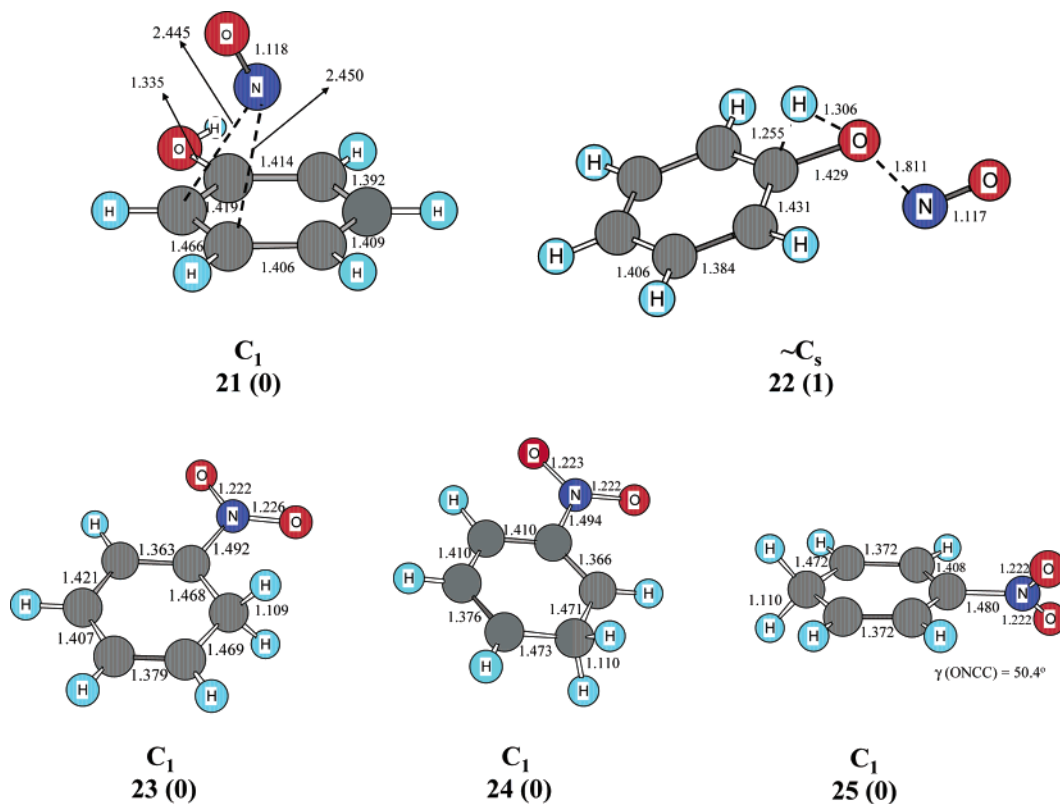


Figure 4. Geometries for products 21–25 of  $\text{NO}_2^+$ /benzene obtained with energy minimization procedures at the B3LYP/6-31++G\*\* level.

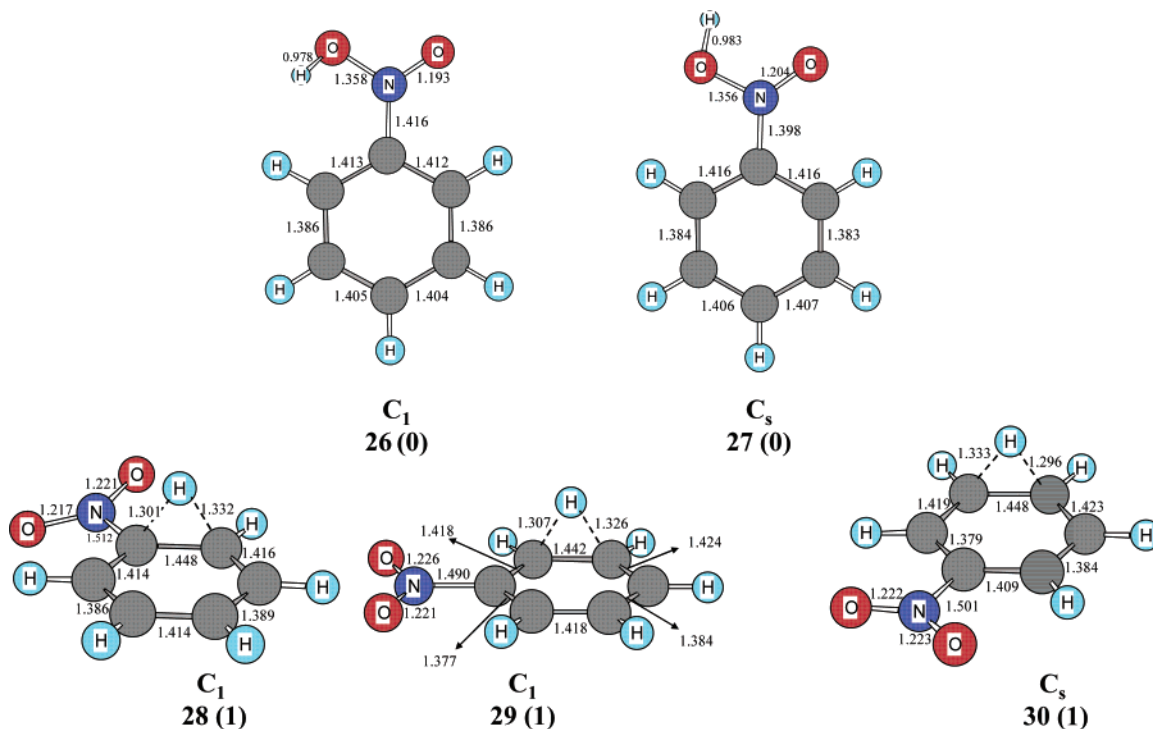
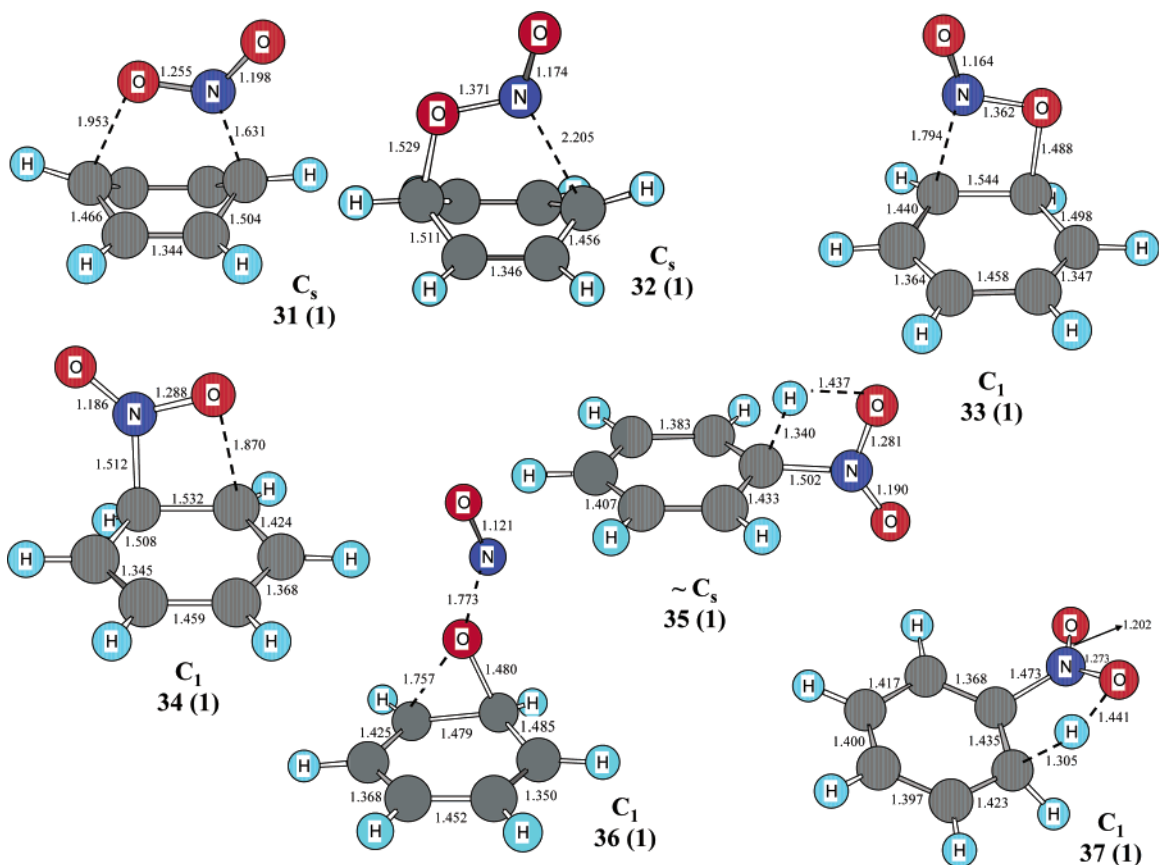


Figure 5. Geometries for products 26–30 of  $\text{NO}_2^+$ /benzene obtained with energy minimization procedures at the B3LYP/6-31++G\*\* level.

nitration of benzene. Particularly significant are **3** and **4**, since these are the intermediates formed prior to  $\sigma$ -complex (**8**) formation. These represent the center of the discussion regarding the nature of the intermediate formed before the reactants collapse to the  $\sigma$ -complex, that is, whether a  $\pi$ -complex or a single-electron-transfer (SET) intimate pair are involved, as proposed originally by Olah<sup>10,11</sup> and Weiss,<sup>18</sup> respectively.

Analysis of our present data leads to the new conclusion that more than one intermediate may be involved prior to the  $\sigma$ -complex formation. Structures **3** and **4** are intermediates that fit respectively into the definition of the  $\pi$ -complex and SET intimate pair. Analysis of the geometry of these two intermediates leads to the conclusion that they are indeed distinct species. Structure **3** is an unoriented (outer)  $\pi$ -complex, whereas **4** can



**Figure 6.** Geometries for the transition states 31–37 connecting the several intermediates, calculated at B3LYP/6-31++G\*\* level.

be also viewed as an oriented  $\pi$ -complex according to Olah's early suggestion for such complexes.<sup>10,11</sup> However, considering more carefully structure **4**, one realizes that the NO<sub>2</sub> moiety is rather bent in relation to **3**, in which this moiety is linear. The O–N–O bond angle in **4** is 136.7°, quite close to the angle of an isolated NO<sub>2</sub> molecule (134.1°),<sup>35</sup> which indicates that NO<sub>2</sub> is strongly interacting with the benzene  $\pi$ -system in **4**. This can be an indication that single-electron transfer from benzene to NO<sub>2</sub><sup>+</sup> has already occurred in this geometry, affording **4**, which is thus an inner sphere or intimate pair SET, single-electron-transfer complex (according to Marcus theory). Analysis of the relative energies of the species (Table 1) indicates that structures **3** and **4** are quite distinct energetically (**3** is 13.6 kcal/mol higher in energy than **4**), which would be unexpected if both were just  $\pi$ -complexes (in which case interactions between the reactants should be similar). It is interesting to point out that structure **4** is only 0.7 kcal/mol higher in energy than the  $\sigma$ -complex **8**. The reaction barrier for the conversion of **4** to **8** is only 0.9 kcal/mol. This could mean that most of the driving force for the reaction to occur is already released in this structure, possibly by single-electron transfer from benzene to the nitronium ion affording the inner sphere complex **4**.

We further investigated the electronic structure of these complexes in order to probe if the best representation for their ground state would be a  $\pi$ -complex or an intimate radical–radical ion pair formed by single-electron transfer. A simple way for this is by the analysis of the charges in different fragments of the complex. ChelpG<sup>36</sup> charge analysis for the

structure of the complex **3** shows that the positive charge is most equally distributed between the NO<sub>2</sub> and benzene (Table 2). The linear NO<sub>2</sub> interacts with the  $\pi$ -aromatic system through oxygen, which besides the central nitrogen atom is the other potential electrophilic center in the NO<sub>2</sub><sup>+</sup> cation but is usually not considered in nitration mechanisms. This is rather in line with the experimental finding of O<sup>+</sup> being transferred in the gas-phase nitration of benzene with NO<sub>2</sub><sup>+</sup>. It is also noteworthy that formation of small amounts of phenol was reported in the HNO<sub>3</sub>/H<sub>2</sub>SO<sub>4</sub> nitration of benzene,<sup>2a</sup> which may stem from competing oxidation involving an oxygen-transfer pathway.

The charge distribution analysis of the “oriented  $\pi$ -complex” (structure **4**), indicates that the positive charge is basically located on the ring, which means that the NO<sub>2</sub> moiety received an electron from the  $6\pi$ -aromatic, resulting in an SET radical–radical ion intimate pair. Therefore, **4** can be better described as an NO<sub>2</sub> radical interacting with a benzene cation–radical, C<sub>6</sub>H<sub>6</sub><sup>•+</sup>. Calculations assume, however, that the NO<sub>2</sub><sup>+</sup> is unencumbered, but in the condensed phase, there is always some interaction with the counterion.

Morokuma decomposition analysis<sup>37</sup> permits us to shed light on the prominent factors in the interaction energy between benzene and NO<sub>2</sub><sup>+</sup>, showing that the main stabilizing contributor

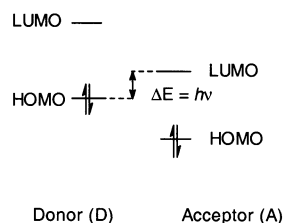
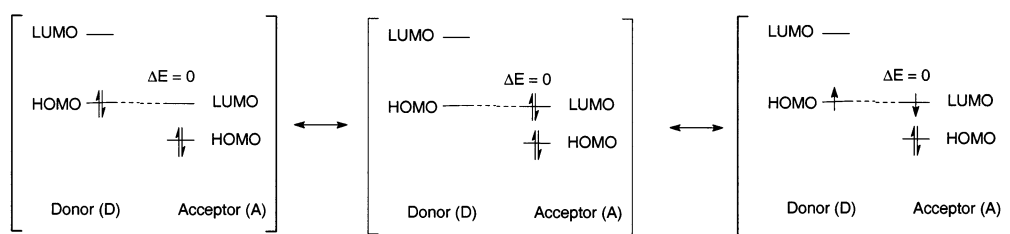
(35) Herzberg, G. *Electronic Spectra and Electronic Structure of Polyatomic Molecules*; Van Nostrand: New York, 1966.

(36) (a) Chirlian, L. E.; Francl, M. M. *J. Comput. Chem.* **1987**, *8*, 894–905. (b) Breneman, C. M.; Wiberg, K. B. *J. Comput. Chem.* **1990**, *11*, 361–373.

(37) See: (a) Coulson, C. In *Hydrogen Bonding*; Hadzi, D., Thompson, H. W., Eds.; Pergamon Press: New York, 1957; pp 339–360. (b) Coulson, C. *Research* **1957**, *10*, 149–159. (c) Morokuma, K. *J. Chem. Phys.* **1971**, *55*, 1236–44. (d) Kitaura, K.; Morokuma, K. *Int. J. Quantum Chem.* **1976**, *10*, 325. (e) Morokuma, K.; Kitaura, K. In *Chemical Applications of Electrostatic Potentials*; Politzer, P., Truhlar, D. G., Eds.; Plenum Press: New York, 1981; pp 215–242.



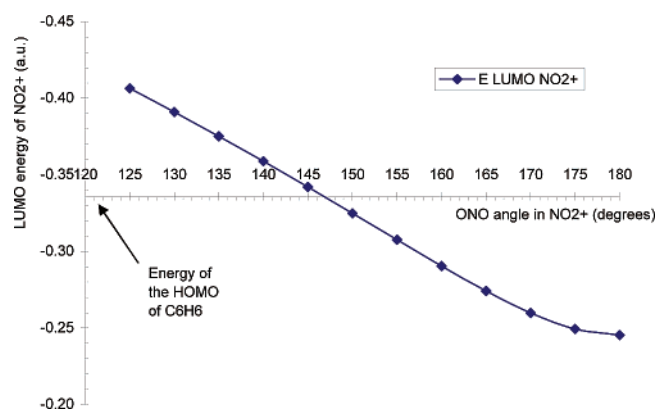
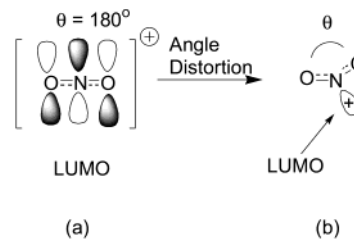


(a) Ground State:  $|\text{NO}_2^+, \text{C}_6\text{H}_6\rangle$ (b) Ground State:  $c_1 |\text{NO}_2^+, \text{C}_6\text{H}_6\rangle + c_2 |\text{NO}_2, \text{C}_6\text{H}_6^+\rangle + \dots$ **Figure 8.** Frontier molecular orbital analysis and its relation with single-electron-transfer nitration.

involving the HOMO and LUMO orbitals of the donor–acceptor complex. Two distinct schemes of the molecular orbital interactions are possible based on the HOMO–LUMO energy gap ( $\Delta E$ ) of the MO's of the complex:  $\Delta E \neq 0$  and  $\Delta E \approx 0$  (Figure 8a,b).

In this approach, the electron transfer is characterized by the case where the HOMO–LUMO gap in the complex is very small ( $\Delta E \approx 0$ ). In the extreme case where  $\Delta E = 0$ , electronically degenerate molecular orbitals result (see Figure 8b). In this regard, it is important to point out that electron-transfer processes are related to the interaction between different electronic surfaces,<sup>31</sup> which are regions of the potential energy surface where the Born–Oppenheimer approximation (adiabatic approximation), common to most ab initio calculations, usually fails. According to Hund's rule, the lowest energy electronic configuration for this case would be achieved by distributing a single electron in each degenerate orbital in order to minimize Pauli electronic repulsion (Figure 8b). This can be characterized as a single-electron transfer. Based on this picture, a charge transfer intermediate is usually a precursor to electron transfer. Complex **3**, considered originally as an unoriented  $\pi$ -complex, could be thus considered as a charge-transfer complex intermediate involving strong electrostatic interaction. Consequently, single-electron transfer from benzene to  $\text{NO}_2^+$  occurs when the HOMO of benzene (electron donor) is approximately at the same energy level as the LUMO of  $\text{NO}_2^+$  (electron acceptor). This could occur upon distortion of the geometry of the reactants. However, analysis of the molecular orbitals of the nitronium ion indicates that its LUMO is related to the empty orbital on nitrogen. Thus, by bending  $\text{NO}_2^+$  from its original linear form, the empty  $sp^2$  formed orbital at the nitrogen atom becomes the main contributor to the LUMO of the molecule (Scheme 6).

This LUMO should become more low-lying in energy as the O–N–O bond angle decreases, whereby resonance stabilization involving the nonbonded electron pairs on the oxygen atoms decreases. The LUMO energy of  $\text{NO}_2^+$  could decrease to a value

**Figure 9.** Plot of the LUMO energy of  $\text{NO}_2^+$  as a function of the O–N–O bond angle. The LUMO of  $\text{NO}_2^+$  becomes isoenergetic with the HOMO of benzene at  $147^\circ$ , indicating an approximate geometry for the SET process.**Scheme 6.** LUMO in  $\text{NO}_2^+$  Cation at (a) Linear and (b) Bent Geometries

where it becomes isoenergetic to the HOMO of benzene, favoring single-electron transfer, according to the model shown in Figure 8b. We performed RHF/6-311++G\*\* single point energy calculations on distorted  $\text{NO}_2^+$  geometries and benzene in order to obtain the HOMO–LUMO values and to gather an estimate of the  $\text{NO}_2^+$  geometry at which SET should take place. The O–N–O bond angle of about  $147^\circ$  renders the LUMO of  $\text{NO}_2^+$  isoelectronic with the HOMO of benzene, at which point electron transfer takes place (Figure 9). Bending  $\text{NO}_2^+$  from linear (ONO bond angle from  $180^\circ$ ) in complex **3** to  $147^\circ$  at

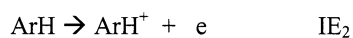
Table 3. Gas-Phase Ionization Potentials<sup>39</sup>

substrate	ionization energy <sup>a</sup> (IE) (eV)	$\Delta$ IE for reaction with $\text{NO}_2^+$ (eV)	$\Delta$ IE for reaction with $\text{NO}_2^+$ (kcal/mol)
$\text{NO}_2 \rightarrow \text{NO}_2^+ + e$	9.586 ± 0.002	0.000	0.00
$\text{NO} \rightarrow \text{NO}^+ + e$	9.2642 ± 0.00002	-0.322	-7.42
benzene $\rightarrow \text{C}_6\text{H}_6^+ + e$	9.24378 ± 0.00007	-0.342	-7.89
nitrobenzene $\rightarrow \text{C}_6\text{H}_5\text{NO}_2^+ + e$	9.94 ± 0.08	+0.354	+8.16
1,2-dinitrobenzene $\rightarrow \text{C}_6\text{H}_4\text{N}_2\text{O}_4^+ + e$	10.71	+1.124	+25.92
1,3-dinitrobenzene $\rightarrow \text{C}_6\text{H}_4\text{N}_2\text{O}_4^+ + e$	10.4	+0.814	+18.77
1,4-dinitrobenzene $\rightarrow \text{C}_6\text{H}_4\text{N}_2\text{O}_4^+ + e$	10.3 ± 0.1	+0.714	+16.5
	10.50 ± 0.02		
	10.63 ± 0.10		
	10.65		
fluorobenzene $\rightarrow \text{C}_6\text{H}_5\text{F}^+ + e$	9.20 ± 0.01	-0.386	-8.90
chlorobenzene $\rightarrow \text{C}_6\text{H}_5\text{Cl}^+ + e$	9.07 ± 0.02	-0.516	-11.9
bromobenzene $\rightarrow \text{C}_6\text{H}_5\text{Br}^+ + e$	9.00 ± 0.03	-0.586	-13.5
iodobenzene $\rightarrow \text{C}_6\text{H}_5\text{I}^+ + e$	8.72 ± 0.04	-0.866	-20.0
$\text{C}_6\text{H}_5\text{CN} \rightarrow \text{C}_6\text{H}_5\text{CN}^+ + e$	9.73 ± 0.01	+0.144	+3.32
$\text{C}_6\text{H}_5\text{CF}_3 \rightarrow \text{C}_6\text{H}_5\text{CF}_3^+ + e$	9.685 ± 0.005	+0.099	+2.28
<i>o</i> - $\text{C}_6\text{H}_4\text{F}_2 \rightarrow \text{o-C}_6\text{H}_4\text{F}_2^+ + e$	9.29 ± 0.01	-0.296	-6.83
<i>m</i> - $\text{C}_6\text{H}_4\text{F}_2 \rightarrow \text{m-C}_6\text{H}_4\text{F}_2^+ + e$	9.33 ± 0.02	-0.256	-5.90
<i>p</i> - $\text{C}_6\text{H}_4\text{F}_2 \rightarrow \text{p-C}_6\text{H}_4\text{F}_2^+ + e$	9.1589 ± 0.0005	-0.427	-9.85
<i>o</i> - $\text{C}_6\text{H}_4\text{Cl}_2 \rightarrow \text{o-C}_6\text{H}_4\text{Cl}_2^+ + e$	9.06 ± 0.02	-0.526	-12.13
<i>m</i> - $\text{C}_6\text{H}_4\text{Cl}_2 \rightarrow \text{m-C}_6\text{H}_4\text{Cl}_2^+ + e$	9.10 ± 0.02	-0.486	-11.21
<i>p</i> - $\text{C}_6\text{H}_4\text{Cl}_2 \rightarrow \text{p-C}_6\text{H}_4\text{Cl}_2^+ + e$	8.92 ± 0.03	-0.666	-15.36
$\text{PhOH} \rightarrow \text{PhOH}^+ + e$	8.49 ± 0.02	-1.096	-25.27
$\text{PhOMe} \rightarrow \text{PhOMe}^+ + e$	8.20 ± 0.05	-1.386	-31.96
toluene $\rightarrow \text{C}_7\text{H}_8^+ + e$	8.828 ± 0.001	-0.758	-17.48
mesitylene $\rightarrow \text{C}_9\text{H}_{12}^+ + e$	8.40 ± 0.01	-1.186	-27.35
$\text{PhNH}_2 \rightarrow \text{PhNH}_2^+ + e$	7.720 ± 0.002	-1.866	-43.03
naphthalene $\rightarrow \text{C}_{10}\text{H}_8^+ + e$	8.1442 ± 0.0009	-1.442	-33.25
	8.141 ± 0.01		
$\text{CH}_4 \rightarrow \text{CH}_4^+ + e$	12.61 ± 0.01	+3.024	+69.73
$\text{C}_2\text{H}_6 \rightarrow \text{C}_2\text{H}_6^+ + e$	11.52 ± 0.04	+1.934	+44.60
$\text{C}_3\text{H}_8 \rightarrow \text{C}_3\text{H}_8^+ + e$	10.94 ± 0.05	+1.354	+31.22
<i>i</i> - $\text{C}_4\text{H}_{10} \rightarrow \text{i-C}_4\text{H}_{10}^+ + e$	10.68 ± 0.11	+1.094	+25.22

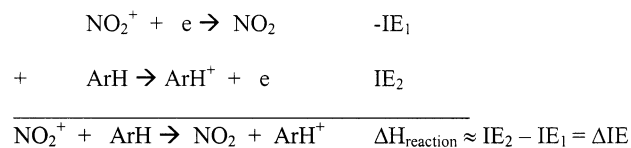
<sup>a</sup> Data from the NIST database (<http://webbook.nist.gov/chemistry>).

this level of calculation raises its energy by about 7 kcal/mol. This value should be considered as the upper limit for the barrier to single-electron transfer from structure 3. An ab initio correlated calculation (MRCI/6-31G) for nitration of toluene predicts that the single-electron transfer should occur at an O–N–O bond angle of approximately 150°,<sup>26</sup> supporting the present model for single-electron transfer. However, due the small size of the basis set utilized in this MRCI study, the geometries obtained are only approximate.

Another aspect to be considered is how readily can an aromatic ring transfer an electron to the  $\text{NO}_2^+$  ion. This is usually considered to be one of the main arguments against the generality of the SET mechanism for electrophilic aromatic nitration.<sup>38</sup> Experimental values for ionization energies (IE) in the gas phase are available and provide some indication to the thermodynamic feasibility of the SET process. The ionization energy (IE) for  $\text{NO}_2$  and aromatics related to the nitration reaction are shown subsequently.



From the experimental values of ionization energies and involved electron-transfer step shown in the equations, it can be deduced that the enthalpy of the SET process is given by differences of ionization energy, as



Experimental data and the  $\Delta$ IE calculated accordingly are summarized in Table 3, showing also related comparative data for  $\text{NO}^+$ .

Based on these data,  $\text{NO}^+$  is indicated to be a lesser oxidizing agent in the gas phase than  $\text{NO}_2^+$ , as shown by the ionization energies of the two ions. This is contrary to the findings based on electrochemical studies.<sup>40</sup> Estimates of the thermodynamics for single-electron-transfer reactions from a series of substrates to  $\text{NO}_2^+$  are shown in Table 3. It can be seen that SET from benzene to the nitronium cation, affording the aromatic cation radical  $\text{ArH}^{+\bullet}$  and neutral  $\text{NO}_2$ , is thermodynamically feasible ( $\Delta$ IE = -0.342 eV = -7.89 kcal/mol). At the same time,  $\text{NO}^+$  is found to be thermodynamically less likely to abstract an electron from benzene in the gas phase ( $\Delta$ IE = -0.020 eV = -0.46 kcal/mol) than the  $\text{NO}_2^+$  ion. This could explain why a persistent  $\pi$ -complex between  $\text{NO}^+$ /benzene can be observed experimentally<sup>41,42</sup> and even be isolated and crystallized,<sup>43</sup> in contrast with the  $\text{NO}_2^+$  where no such complex is observed.

(39) Data from the NIST database (<http://webbook.nist.gov/chemistry>).

(40) Ebersson, L.; Radner, F. *Acta Chem. Scand.* **1984**, *B38*, 861.

(41) (a) Kim, E. K.; Kochi, J. K. *J. Am. Chem. Soc.* **1991**, *113*, 4962. (b) Rosokha, S. V.; Kochi, J. K. *J. Am. Chem. Soc.* **2001**, *123*, 8985–8999.

(42) Schmitt, R. J.; Buttrill, S. E., Jr.; Ross, D. S. *J. Am. Chem. Soc.* **1984**, *106*, 926.

(43) Hubig, S. M.; Kochi, J. K. *J. Org. Chem.* **2000**, *65*, 6807–6818.

(38) See ref 2a, p 199.

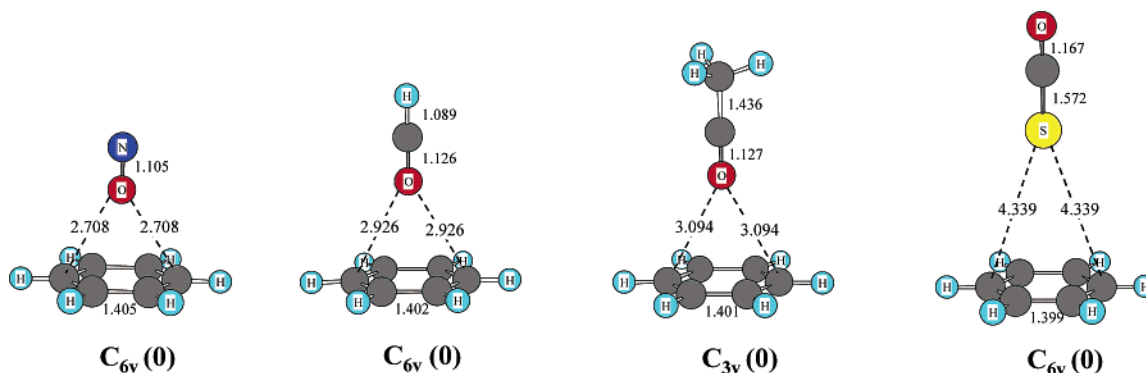


**Figure 10.** Electrostatic complexes formed by the interaction of benzene with related electrophiles and model compound COS.

Activation of strongly deactivated aromatics such as nitrobenzene and trifluoromethylbenzene ( $C_6H_5CF_3$ ) as well as that of alkanes via single-electron transfer to the nitronium cation is, however, unfavorable ( $\Delta IE > 0$ ). Nevertheless, halobenzenes and dihalobenzenes are indicated to be able to undergo oxidation by  $NO_2^+$  ( $\Delta IE < 0$ ) through a SET mechanism, which could alternatively explain the observed unusual *ortho/para* selectivity in their electrophilic nitrations.<sup>44</sup> It should be pointed out that solvent effects and interaction with the counterion can change the ionization energies, especially for the nitronium ion; this could result in thermodynamically favorable gas-phase reactions becoming unfeasible or vice-versa. It is therefore reasonable to expect that these effects could change the mechanism from an SET to a polar two-electron-transfer reaction, and their role should not be ignored.

If the rate-determining step involves electron transfer, isotope effects should not affect the rate (if one considers the models of nonlocalized electrons and vertical transitions); thus,  $k_H/k_D$  should be 1. Using ICR techniques for studying these reactions in the gas phase, Olah and co-workers found no isotope effect (i.e.,  $k_H/k_D = 1$ ).<sup>30</sup> This could mean that the reaction is driven in this case by single-electron transfer. Olah and collaborators have also shown that the nitration of benzene and its isotopomers with  $NO_2^+BF_4^-$  salts in  $CH_2Cl_2$  solution gave an inverse secondary isotopic effect ( $k_H/k_D = 0.86$ ).<sup>45a-c</sup> Hence, a single-electron-transfer mechanism cannot be the rate-determining step in this case. It follows that the lowest energy path in the gas phase and in solution may involve differing rate-determining steps. Since substrate selectivity is also low in this case, the rate-determining step is considered to be the formation of the electrostatic donor-acceptor complex, proposed originally by Olah<sup>2a</sup> as the unoriented  $\pi$ -complex.

**Interaction of Benzene with Other Electrophiles and Model Compounds.** To better understand the effect of electrostatic interactions, we subsequently performed DFT calculations of the interaction between benzene with other electrophiles that configurationally resemble  $NO_2^+$ , namely  $NO^+$ ,  $CO_2$  (isoelectronic to  $NO_2^+$ ), and acetyl and formyl cations ( $H_3C-CO^+$ ,  $HCO^+$ ) as well as the model molecule COS. Complexes which were characterized as minima are shown in Figure 10. A recent theoretical study by Heidrich<sup>45d</sup> has shown that whereas the isopropyl cation with benzene forms a  $\sigma$ -complex as the

only intermediate, the *tert*-butyl cation with benzene was found to form a  $\pi$ -complex in addition to a  $\sigma$ -complex as distinct intermediates. An infrared report in the gas phase<sup>45e</sup> on protonated benzene has shown the  $\sigma$ -complex as the stable intermediate in agreement with the condensed phase studies.

The data in Figure 10 illustrate that the neutral COS with a nonzero dipole moment, as well as related charged species ( $NO^+$ ,  $HCO^+$ , and  $H_3CCO^+$ ), form adducts with benzene in which the interaction takes place through the oxygen atom leading to a minima on their respective potential energy surfaces, similar to what was found for structure 3. On the other hand,  $CO_2$ , isoelectronic with the nitronium cation, does not form a stable complex in a “T” configuration at the B3LYP level, inferring that the positive charge character and polarizability of the nitronium ion is a fundamental driving force for its attraction to the aromatic ring. Such an interaction is probably of an electrostatic nature and may be responsible for the initial approach between the electrophile and the aromatic substrate. As this is a long-range interaction, it should be somewhat insensitive to the substrates’ structure, and this may explain the low substrate selectivity found for nitrations with the nitronium salts. The interaction via the oxygen atom of the electrophile, or by sulfur, in COS, raises the possibility that they may also act as ambident electrophiles. In the case of  $NO_2^+$ , this would ultimately lead to oxygen transfer, as was observed in the gas phase. Increasing the nucleophilicity of the substrates lead to stronger interactions. For example, in the reaction of  $NO_2^+$  with ethylene, a stronger  $\pi$ -donor than benzene, this interaction could be significantly augmented. Actually, Cacace et al. performed gas-phase ICR measurements<sup>47</sup> on the reaction of ethylene with  $NO_2^+$  and observed a rearranged product that was suggested to be derived from the *O*-nitroso adduct, probably  $CH_3CHO-NO^+$ . These results were supported by high level ab initio calculations, which show that structures VI, VIII, IV, I, V, XIV, and XV (original numbering from ref 48; see Figure 11) are the only species found on the potential energy surface as minima.<sup>48</sup> Structure V is the *O*-nitroso complex of oxirane which may originate from oxygen transfer by  $NO_2^+$  to ethylene, supporting the existence of an O-oriented  $\pi$ -complex. The obtained theoretical results and experimental data from ICR measurements validate this model.

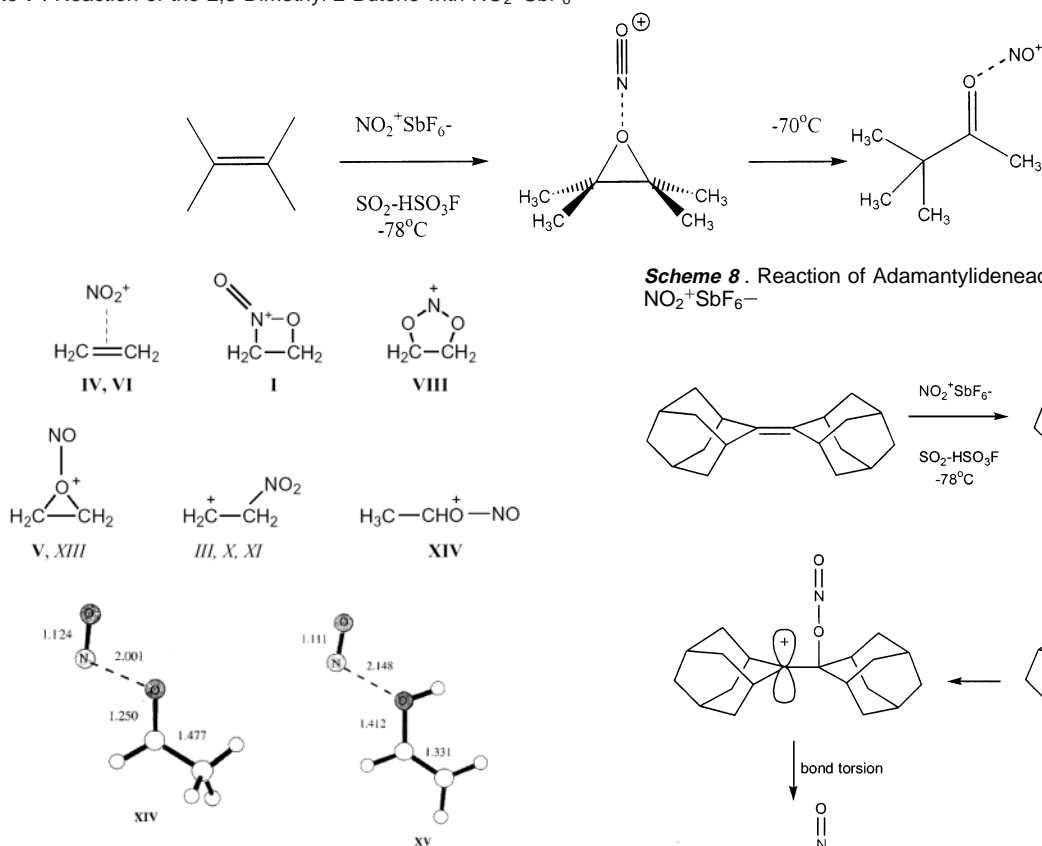
(44) See ref 4a, p 509–510.

(45) (a) Reference 2a, p 140. (b) Hunziker, E.; Myhre, P. C.; Penton, J. R.; Zollinger, H. *Helv. Chim. Acta* **1975**, *58*, 230. (c) Olah, G. A. *J. Tenn. Acad. Sci.* **1965**, *40*, 77. (d) Heidrich, D. *Angew. Chem., Int. Ed.* **2002**, *41*, 3208. (e) Solcà, N.; Dopfer, O. *Angew. Chem., Int. Ed.* **2002**, *41*, 3628.

(46) (a) Reference 11, p 247, using Mulliken definition. (b) Mulliken, R. S. *J. Am. Chem. Soc.* **1950**, *72*, 600. (c) Mulliken, R. S. *J. Am. Chem. Soc.* **1952**, *74*, 811. (d) Mulliken, R. S. *J. Phys. Chem.* **1952**, *56*, 801.

(47) Cacace, F.; de Petris, G.; Pepi, F.; Rossi, I.; Venturini, A. *J. Am. Chem. Soc.* **1996**, *118*, 12719–12723.

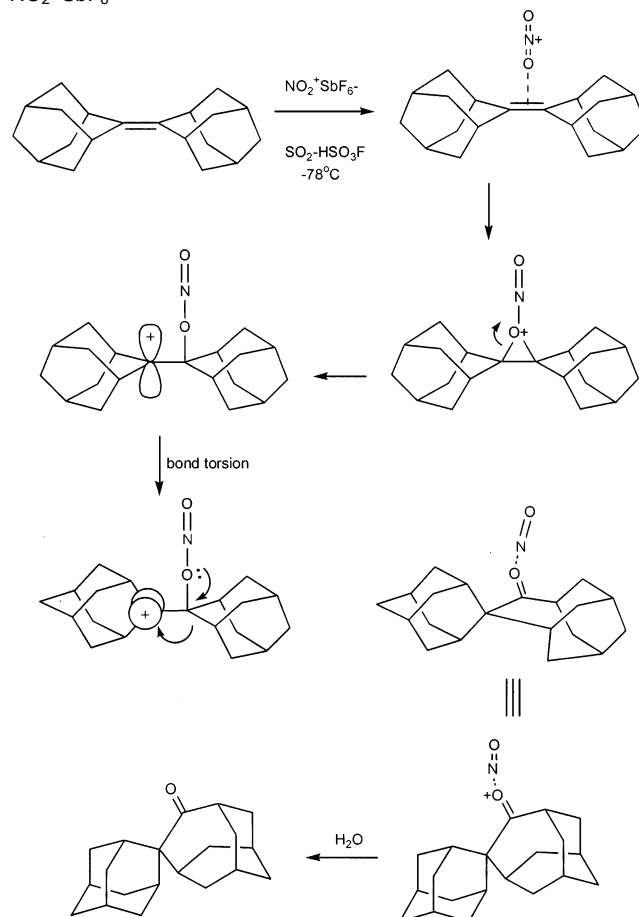
(48) Bernardi, F.; Robb, M. A.; Rossi, I.; Venturini, A. *J. Org. Chem.* **1993**, *58*, 7074–7078.

**Scheme 7.** Reaction of the 2,3-Dimethyl-2-Butene with  $\text{NO}_2^+\text{SbF}_6^-$ **Figure 11.** Structures VI, VIII, IV, I, V, XIV, and XV from ref 48.

**Reaction of Alkenes with  $\text{NO}_2^+$ .** In their studies of nitration of alkenes with  $\text{NO}_2^+$  salts,<sup>49a</sup> Olah and collaborators found that 2,3-dimethyl-2-butene reacts with  $\text{NO}_2^+\text{SbF}_6^-$  in an  $\text{SO}_2/\text{HSO}_3\text{F}$  solution at  $-78^\circ\text{C}$  to form a “ $\pi$ -complex” which gave a singlet in the  $^1\text{H}$  NMR at  $\delta$  2.42, deshielded by 1.1 ppm from the parent alkene. The “ $\pi$ -complex” was unstable even at  $-70^\circ\text{C}$  and upon standing rearranged to give *O*-nitroso pinacolone (Scheme 7), in a way similar to what was observed in the ICR experiments of the nitration of ethylene.

Related observations were made in the case of sterically crowded alkene, adamantylideneadamantane with  $\text{NO}_2^+\text{SbF}_6^-$  under similar reaction conditions (Scheme 8).<sup>49a</sup>

These results were originally interpreted in terms of a three-center two-electron bond interaction involving the nitrogen atom of  $\text{NO}_2^+$  and the alkene double bond, followed by cationic rearrangement. Alternatively, this process could be understood by  $\text{O}^+$  transfer from  $\text{NO}_2^+$  ion to the olefin, forming an *O*-nitroso epoxide which can rearrange to the observed products without necessarily involving a  $\pi$ -complex with a specific interaction on the nitrogen atom of the  $\text{NO}_2^+$  ion. Indeed, if the interaction occurs through the oxygen atom of  $\text{NO}_2^+$ , as predicted by quantum chemical calculations, the experimental data could be readily rationalized. Recently, it was reported by Kochi, Schleyer et al. that adamantylideneadamantane and sesquihomoadamantane could undergo a electrophilic reaction through a single-electron-transfer mechanism, affording radical cations, which can be intercepted by rapid oxygen transfer from dioxygen, affording the respective epoxides.<sup>49b</sup>

**Scheme 8.** Reaction of Adamantylideneadamantane with  $\text{NO}_2^+\text{SbF}_6^-$ 

**Protonation of Nitrobenzene.** We have also considered the question of the protonation of nitrobenzene because of the microscopic reversibility principle. Our results indicate that nitrobenzene should be protonated at the nitro oxygen (*O*-protonation) rather than on carbon (*C*-protonation; at either *ipso*, *ortho*, *meta*, or *para* positions), since ring protonation is thermodynamically unfavorable by about 30 kcal/mol. The calculated proton affinity of nitrobenzene affording species **27** (192.2 kcal/mol) agrees well with the observed gas-phase experimental value (195.5 kcal/mol<sup>39</sup>), indicating a probable *O*-protonation. Indeed, formation of  $\text{ArNO}_2\text{H}^+$  in solution has been shown under stable ion conditions.<sup>50</sup> Alternative reaction pathways leading to products other than the protonated nitrobenzene were also investigated. These pathways correspond to the addition of  $\text{NO}_2^+$  to benzene through the oxygen atoms. The main reactions are electrocyclic additions leading to species such as **16**, **17**, **18**, **20**, and **21** [ $\text{PhOH}\cdot\text{NO}^+$ ] (Figures 3 and 4)

(49) (a) Olah, G. A. *J. Am. Chem. Soc.* **1974**, *96*, 3581–3589. (b) Rathore, R.; Lindeman, S. V.; Zhu, C.-J.; Mori, T.; Schleyer, P. v. R.; Kochi, J. K. *J. Org. Chem.* **2000**, *65*, 6807–6818 and references therein.

(50) Olah, G. A.; Laali, K. K.; Wang, Q.; Prakash, G. K. S. *Onium Ions*; Wiley: New York, 1998; Chapter 2.

which can undergo rearrangements to produce the oxygen transfer products **14** and **15**. These structures correspond to conformers of benzene oxide complexed to an  $\text{NO}^+$  moiety. Decomposition of these species into a benzene oxide cation and  $\text{NO}$  is shown to be energetically unfavorable (41.2 kcal/mol, from **15**). However, these species correspond to isomers of a complex between phenol and  $\text{NO}^+$ , which links this potential energy surface with that of the nitrosation of phenol. Structure **15** can undergo rearrangement through transition state **22** affording the complex  $[\text{PhOH}\cdot\text{NO}]^+$  (structure **21**). Analysis of this structure indicates that it correspond to a charge-transfer complex between phenol and  $\text{NO}^+$ . This was found to be the most stable minimum on the potential energy surface. Analysis of the charge in the moieties and the  $\text{NO}$  bond length (1.118 Å in the complex, 1.073 Å in  $\text{NO}^+$ , and 1.158 Å in neutral  $\text{NO}$ ) indicates that the positive charge is located on the aromatic ring ( $q_{\text{CHelpG}}(\text{NO}) = +0.32$ ;  $q_{\text{CHelpG}}(\text{PhOH}) = +0.68$ ). Decomposition of **21** leads to  $\text{PhOH}^+$  (a cation radical) and neutral  $\text{NO}$ , in agreement with experimental results.<sup>41a,51</sup> This finding explains why the unsolvated  $\text{NO}_2^+$  cation reacts with benzene to give mainly  $\text{C}_6\text{H}_6\text{O}^+$  product in the gas phase and is in line with a model that the interaction between these two species in the gas phase occur initially through the oxygen atom, as in structure **3**, leading to the products resembling electrocyclic addition products (structures **16** to **20**) which could rearrange to a  $\text{C}_6\text{H}_6\text{O}^+$  product (phenol cation radical). Other epoxide-like structures were also investigated. These rearrangements are predicted to be more facile than conversion to the nitrated product, as observed by the relatively low reaction barriers in the former, compared with pathways that lead to the nitrated product.

## Conclusions

The initial interaction of benzene with a nitronium cation could either involve an initial single-electron transfer or a polar conventional two-electron-transfer electrophilic mechanism, involving a  $\pi$ -complex, since both intermediates are minima on the potential energy surface. The rate-determining step could be either the formation of the first complex or the electron transfer, depending on the system and experimental conditions. This reconciles previous mechanistic proposals, with a better understanding of the role for each of these species. Whereas experimental differentiation between these two intermediates is presently difficult, new experimental techniques such as very fast femtosecond spectroscopy could be useful in the investigation of the reaction.

The mechanistic model proposed herein is analogous to the model proposed by Kochi in a recent perspective,<sup>52</sup> wherein he suggests the existence of a preorganization step involving metastable charge-transfer complexes as precursors to electrophilic aromatic substitution reactions. Using his terms, structure **3** would be a precursor complex (PC), which forms a “successor complex” (SC), which would be **4**. The latter then reacts to give the  $\sigma$ -complex. This proposal is fully supported by our calculations and represents a similar conclusion reached from a different perspective concerning the mechanism of electrophilic aromatic nitration and related reactions.

In summary, based on insights gained via quantum chemical calculations for the reaction of the nitronium cation with benzene, a modified mechanistic scheme is proposed in which three intermediates are involved in the electrophilic nitration of aromatics. The initial T-shaped  $\pi$ -complex **3** would be formed due to an electrostatic interaction between the nitronium ion and the aromatic, in which one of the oxygen atoms of  $\text{NO}_2^+$  interacts with the arene. The second intermediate is formed after single-electron transfer from the aromatic to the nitronium ion in the first complex (a donor/acceptor complex) and has the characteristics of an intimate pair of the aromatic cation-radical/ $\text{NO}_2$  (structure **4**). The complex **4** then collapses via transition state **10** to give the conventional  $\sigma$ -complex **8** (Wheland intermediate). The proposed mechanism involving three intermediates (electrostatic bonded  $\pi$ -complex, radical-ion pair and the  $\sigma$ -complex) for the nitration of “oxidizable” aromatics (by  $\text{NO}_2^+$ ) reconciles previous mechanistic models involving only two intermediates ( $\pi$ -complex or radical-ion pair and the  $\sigma$ -complex) as limiting cases for this mechanism. The relative importance of this mechanism and the conventional polar mechanism will vary depending on the solvent, on experimental conditions, and on the oxidation potential of the substrate. Dependent on these, both pathways are feasible or one of them could predominate.

In the absence of counterion and solvation effects, oxygen transfer from  $\text{NO}_2^+$  to the aromatics takes place in the gas phase leading to charge-transfer complexes between  $\text{C}_6\text{H}_6\text{O}^+$  and  $\text{NO}$  moieties. In this case, the charge-transfer complex between phenol and  $\text{NO}^+$ , which has the appearance of a  $\pi$ -complex, is the most stable species on the potential energy surface. These are also the products observed from the reaction of  $\text{NO}_2^+$  and benzene in the gas phase (ICR studies), corroborating the theoretical results.

## Computational Details

Calculations were performed at the B3LYP/6-311++G\*\*//B3LYP/6-31++G\*\* level,<sup>53</sup> using the Gaussian 98 program.<sup>54</sup> Geometries of all species investigated were fully optimized, and they were characterized as intermediates or transition states on the potential energy surface by the absence or presence of imaginary frequencies, respectively, after vibrational analysis on the optimized geometries. Zero-point energies (ZPE) and thermal corrections at 298 K were calculated utilizing the frequencies calculated at the B3LYP/6-31++G\*\* level. In some cases, it was necessary to perform geometry optimization at the MP2/6-31+G\* level in order to obtain geometries that could not be obtained by the DFT method (these have a star sign (\*) as label). These were characterized as minima or transition states by MP2 vibrational analysis, and their energies were calculated at the B3LYP/6-311++G\*\*//MP2(fc)/6-31+G\*level.

Relative energies were computed and refer to enthalpy differences at 298 K, if not stated otherwise. Single-point energy calculations were

(51) (a) Reents, W. D., Jr.; Freiser, B. S. *J. Am. Chem. Soc.* **1980**, *112*, 271–276. (b) Reents, W. D., Jr.; Freiser, B. S. *J. Am. Chem. Soc.* **1981**, *113*, 2791–2797.

(52) Rosokha, S. V.; Kochi, J. K. *J. Org. Chem.* **2002**, *67*, 1728–1737.

(53) (a) Becke, A. D. *J. Chem. Phys.* **1993**, *98*, 1372. (b) Lee, C.; Yang, W.; Parr, R. G. *Phys. Rev. B* **1988**, *37*, 785.

(54) Frisch, M. J.; Trucks, G. W.; Schlegel, H. B.; Scuseria, G. E.; Robb, M. A.; Cheeseman, J. R.; Zakrzewski, V. G.; Montgomery, J. A., Jr.; Stratmann, R. E.; Burant, J. C.; Dapprich, S.; Millam, J. M.; Daniels, A. D.; Kudin, K. N.; Strain, M. C.; Farkas, O.; Tomasi, J.; Barone, V.; Cossi, M.; Cammi, R.; Mennucci, B.; Pomelli, C.; Adamo, C.; Clifford, S.; Ochterski, J.; Petersson, G. A.; Ayala, P. Y.; Cui, Q.; Morokuma, K.; Malick, D. K.; Rabuck, A. D.; Raghavachari, K.; Foresman, J. B.; Cioslowski, J.; Ortiz, J. V.; Stefanov, B. B.; Liu, G.; Liashenko, A.; Piskorz, P.; Komaromi, I.; Gomperts, R.; Martin, R. L.; Fox, D. J.; Keith, T.; Al-Laham, M. A.; Peng, C. Y.; Nanayakkara, A.; Gonzalez, C.; Challacombe, M.; Gill, P. M. W.; Johnson, B. G.; Chen, W.; Wong, M. W.; Andres, J. L.; Head-Gordon, M.; Replogle, E. S.; Pople, J. A. *Gaussian 98*, revision A.7; Gaussian, Inc.: Pittsburgh, PA, 1998.

performed at the GVB-CASSCF level,<sup>55</sup> using the 6-311++G\*\* basis set at the DFT geometry. The N–O single bonds were coupled in one GVB pair each, and the NO<sub>2</sub>  $\pi$ -bonding and antibonding orbitals were put in a separate block. The six remaining benzene  $\pi$ -electrons were included in the CASSCF(6,6) block. After calculation, bond localization, according to the Edmiston–Ruedenberg localization procedure, was performed.<sup>56</sup> Among the localized orbitals, we can recognize two that could be directly involved in the electron transfer process: one is localized on the carbon, and the other, on the nitrogen directly above. These two CASSCF-localized orbitals are nonorthogonal and almost singly occupied, being consistent with our proposal of an SET mechanism.

The Morokuma energy decomposition analysis was performed at the RHF/6-311G\*\*//B3LYP/6-31+G\* level. The CASSCF single-point energy calculation and Morokuma energy decomposition analysis<sup>37</sup> were performed using the GAMESS-US package.<sup>57</sup>

**Acknowledgment.** For support of our work, the National Science Foundation and Loker Hydrocarbon Research Institute are gratefully acknowledged. P.M.E. acknowledges W. Bruce Kover for helpful discussions and CNPq (PROFIX) and FAPERJ (Brazil) for financial support. K.L. acknowledges partial support from the NIH (1R15CA78235-01A1) and the Loker Hydrocarbon Research Institute for a summer research visit. J.W.M.C. acknowledge financial support from CNPq.

**Supporting Information Available:** Table containing absolute energies, zero-point energies, and thermal corrections for the species discussed in the text. This material is available free of charge via the Internet at <http://pubs.acs.org>.

JA021307W

(55) Clifford, S.; Bearpark, M. J.; Robb, M. A. *Chem. Phys. Lett.* **1996**, *255*, 320.

(56) (a) Edmiston, C.; Ruedenberg, K. *Rev. Mod. Phys.* **1963**, *35*, 457–465. (b) Raffanetti, R. C.; Ruedenberg, K.; Janssen, C. L.; Schaefer, H. F. *Theor. Chim. Acta* **1993**, *86*, 149–165.

(57) (a) Schmidt, G. M. W.; Baldrige, K. K.; Boatz, J. A.; Elbert, S. T.; Gordon, M. S.; Jensen, J. H.; Koseki, S.; Matsunaga, N.; Nguyen, K. A.; Su, S. J.; Windus, T. L.; Dupuis, M.; Montgomery, J. A. *J. Comput. Chem.* **1993**, *14*, 1347–1363. (b) Ivanic, J.; Ruedenberg, K. *Theor. Chim. Acta* **2001**, *106*, 339.